CILAMCE 2017
Florianópolis - Santa Catarina - Brazil

AN ENRICHED AND ADAPTIVE ALGORITHM FOR FREE VIBRATION OF BARS USING NURBS APROACH

Mateus Rauen

Roberto Dalledone Machado

Marcos Arndt

mateusrauen@gmail.com

Universidade Federal do Paranaá, Programa de Pos-Graduação em Métodos Numéricos em Engenharia

R. Cel. Francisco Heraclito dos Santos, 210, Jardim das Américas, Zip Code 81531-990 Curitiba, Paraná, Brazil ?

Abstract. *The purpose of this work is to present an adaptive and enriched view for the vibration phenomenon of bars and trusses in a CAD mapping context. By the use of NURBS shape functions as partition of unity and the geometry exactness with global mapping, descendant from isogeometric concept, a pure isogeometric formulation for bars is proposed. The GFEM philosophy for free vibration analysis is presented and a NURBS based formulation is proposed. Based on numerical experiments, the efficacy of the presented algorithm is tested considering convergence and frequency error spectra. The NURBS based algorithm presents flexibility to change partition of unity parameters and the advantage to describe a global behavior as a local parametric function.*

Keywords: *Isogeometric, NURBS, Enriched Methods, FEM*

1 INTRODUCTION

In the state of art of numerical methods in the last decade isogeometric analysis was introduced as an unification method between FEA (Finite Element Analysis) and CAD (Computer Aided Design) systems due the application of NURBS functions in numerical models Hughes et al. (2005). In the first developments performed by Cottrell et al. (2006) in structural dynamics AIG demonstrated advantages related with the high continuity property of the NURBS functions, which led to accurate frequency spectra when compared with finite element method (FEM). Extended studies considering the application for reissner-mindlin plates and shells Benson et al. (2010a), Thai et al. (2012), thin plates Shojaee et al. (2012) and framed structures Rauen et al. (2017), reinforces IGA advantages related with convergence and also implementation aspects.

Besides the diferent refinements and other convergence improvements the enrichment strategy presented by GFEM/PUFEM/XFEM obtained successful results. Concerning the application of these enriched methods in structural dynamics the works of Arndt et al. (2011), Torii et al. (2015) and Arndt et al. (2016) demonstrates the advantages of GFEM in terms of convergence and accuracy.

The first discussions and steps forward in the unification between the enrichment strategy of GFEM/XFEM/PUFEM was performed by Benson et al. (2010a). Applications for fracture mechanics Luycker et al. (2011) and propagating cracks Ghorashi et al. (2011) demonstrated advantages related with numerical efficiency of NURBS partition of unity and implementation aspects related to mesh creation and refinement, from CAD representation.

Due this advantage from CAD representations many discussions and tests of IGA were performed for 2D tests. However some tests and formulations of IGA concerning unidimensional elements remains not yet discussed on the literature. Furthermore the applications of enriched isogeometric analysis for structural dynamics were not yet been tested. This paper aims to propose and test a pure and enriched formulation concerning the free vibration problem of CAD mapped bars.

2 ISOGEOMETRIC ANALYSIS

Isogeometric analysis (IGA) is discrete numerical method to solve partial diferential equations where the domain analysis is exactly described by NURBS functions, from CAD classical literature Farin (1999), Piegl and Tiller (1997). Like FEM, IGA is also origined by an weighted formulation and discretization. The most remarkable diference between IGA and FEM is in the discretization strategy Hughes et al. (2005). The usual implementation of FEM is to divide the physical domain in a finite number of locally mapped isoparametric elements. Figure 1 shows the classical FEM mesh mapping strategy, with a local context of mapping and global node coupling. Isogeometric analysis adopts the global mapping concept where the whole parametric space is mapped to the physical domain. Figure 2 shows the basic IGA strategy. Is important to note that FEM performs the discretization process in the physical domain, while IGA performs the discretization in the parametric domain which allows the global mapping by NURBS exact describing geometry.

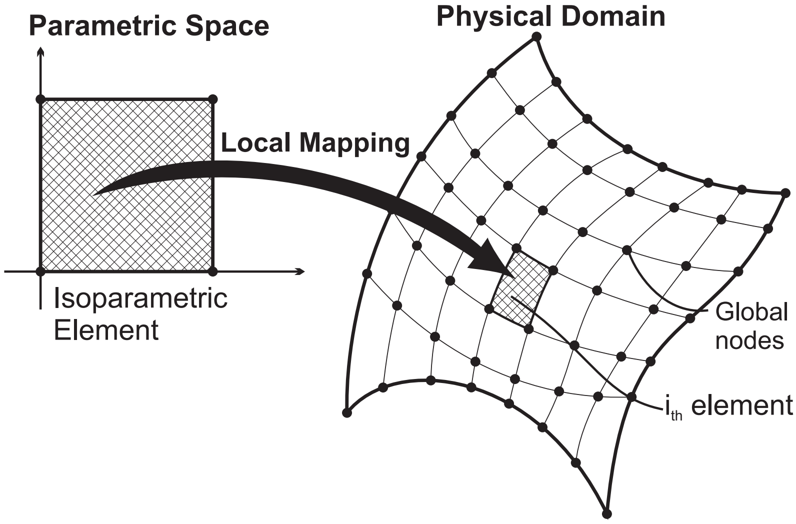

Figure 1: Classical mapping scheme in FEM

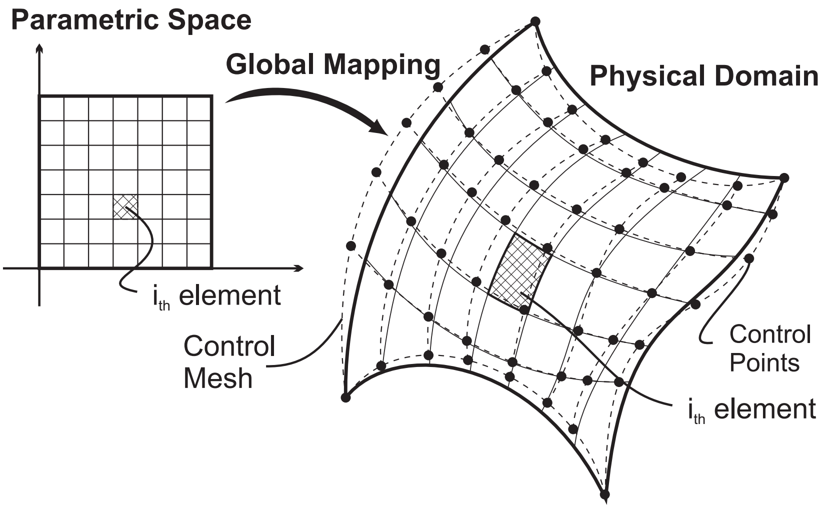

Figure 2: IGA mapping strategy

2.1 B-spline shape functions

The fundamental functions to create the solution and geometric space in isogeometric analysis are the b-splines shape functions. In parametric space, the subdivision of elements is performed by the knots concept. These knots consists in a set of coordinates in the parametric space which holds the number of functions and its continuity. The b-splines shape functions is a set of parametric polynomials defined by a polynomial degree p and a set of knots $\Xi = \{\xi_1, \xi_2, \ldots, \xi_{n+p+1}\}$ where knots can appear repeatedly but in an ascending order, and n is the number of b-splines shape functions. The shape functions are recursively defined by De-Boor (1972):

$$N_{i,0}(\xi) = \begin{cases} 1 & \text{if } \xi_i \leq \xi < \xi_{i+1}, \\ 0 & \text{otherwise} \end{cases}, \tag{1}$$

starting from an null degree iteration. The iteration for p_{th} degree is given by:

$$N_{i,p}(\xi) = \frac{\xi - \xi_i}{\xi_{i+p} - \xi_i} N_{i,p-1}(\xi) + \frac{\xi_{i+p+1} - \xi}{\xi_{i+p+1} - \xi_{i+1}} N_{i+1,p-1}(\xi). \tag{2}$$

The b-splines shape functions has some important properties. Namely:

- 1) The continuity of the b-splines set in the knot ξ_i are related with its multiplicity in Ξ, i.e the functions have $p - m_i$ continuous derivatives at the knot ξ_i, where m_i is the knot multiplicity;
- 2) The support of a NURBS shape function $N_{i,p}$ is defined in the interval $[\xi_i, \xi_{i+p+1}]$;
- 3) The b-splines shape functions follows the partition of unity in parametric space, i.e $\sum_{i=1}^{n} N_{i,p}(\xi) = 1$.

The usual knot configuration in isogeometric analysis is to use the open concept Farin (1999), i.e $p + 1$ edge knots. Interior knots also controls the continuity, being that ξ_i repeated p times created an C^0 continuity in that point.

2.2 Curve representation and NURBS functions

A curve defined in a physical domain is mapped by a set o b-splines shape functions by the relation:

$$\mathbf{C}(\xi) = \sum_{i=1}^{n} N_{i,p}\,\mathbf{B}_i, \tag{3}$$

where $\mathbf{B}_i$ is the i_{th} control point set which defines the curve.

Non uniform rational b-splines (NURBS) functions are originated from b-splines, to increase CAD representation of objects. The control points, used to map a curve in a physical domain appear weighted, being possible to represent a more complex curve than a *beziér* curve Piegl and Tiller (1997). The NURBS functions are defined as a weighted rational set $R_{i,p}$, based in a b-spline set $N_{i,p}$. Given a set of n control points $\mathbf{B}$ and a set of n weights $\mathbf{w}$, NURBS set is the defined as:

$$R_{i,p} = \frac{N_{i,p}\,w_i}{\sum_{\hat{i}=}^{n} N_{\hat{i},p}\,w_{\hat{i}}}. \tag{4}$$

A curve origined by a NURBS set is defined by:

$$\mathbf{C}(\xi) = \sum_{i=1}^{n} R_{i,p}\,\mathbf{B}_i. \tag{5}$$

The insertion of weights and the rational concept implied a more flexible possibility to perform curves construction, being possible to control curvature radius, which comes from the projective concept given by weights Farin (1999). From a practical view of implementation in isogeometric analysis (fig. 3), the construction of a NURBS curve can be though as a transformation which maps a point in the parametric space ξ directly to the physical space $\mathbf{C} = (x, y)$.

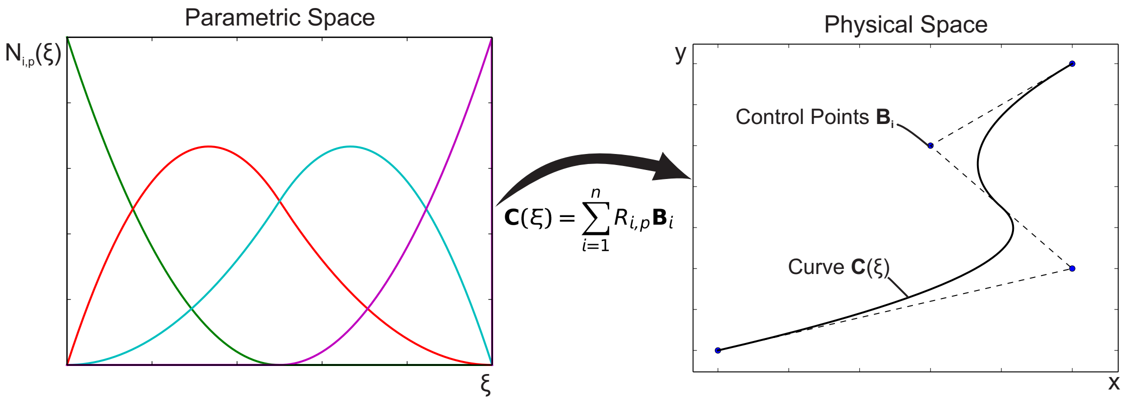

Figure 3: Basic NURBS curve mapping scheme

2.3 Refinements in IGA and CAD

Refinement procedures in IGA are related with the modifications of the parameters Ξ (knot vector) and p (polynomial degree). In CAD procedures, several refinement techniques are discussed and exampled by Piegl and Tiller (1997) aiming to locate control points and weights properly by impose equality in curve equations. These algorithms implies in automatic mesh refinement.

Considering NURBS curve refinement in isogeometric analysis, three kind of basic refinement procedures are possible to perform (Cottrell et al., 2007), namely: *h* refinement, *p* refinement and *k* refinement. Like FEM, IGA *h* refinement is related with point increasing without change polynomial degree. In IGA this means to add new knots in the knot vector and recompute the functions, by the recursive formula (eqs. 1,2) and the points and weights by the algorithms given by Piegl and Tiller (1997). This results in a higher amount of b-splines shape functions, control points, weights and degrees of freedom in the system. Refinements *k* and *p* are related with knot vector changing and also polynomial degree increasing. The basic difference between these refinements techniques is that *p* refinement performs the polynomial degree increasing aiming to maintain b-spline shape functions continuity at certain knots, a necessary procedure to maintain some kind of geometries like squares and cusps. An detailed guide about geometry and mesh procedures in NURBS construction is given by Farin (n.d.). Refinement *k* is related with degree elevation followed by knot insertion, which generates higher continuity functions at the knots. Several works present the advantage of *k* refinement over *p* and *h* refinements in terms of convergence, due mostly to its continuity growing (property 1 of eqs. 1 and 2) with fewer degrees of freedom than *p* refinement (Cottrell et al., 2007, Hughes et al., 2005). In structural dynamics the works of Cottrell et al. (2006) and recently Rauen et al. (2017) reinforce this statement.

3 Dynamic response formulation for CAD mapped bars

3.1 Pure isogeometric formulation

The differencial equation which describes the equilibrium of an undamped system in a global domain C comes from dynamic equilibrium imposing in a straight differencial (Petyt, 2010), as shown in figure 4 which represents the free body forces in an infinitesimal element of curve **C**. Under a time dependent force $p(\mathbf{C}, t)$, the structure response in terms of axial forces N is described in terms of displacements $\bar{u}$ considering a linear elastic condition. The inercial mass force $f_i(\mathbf{C}, t)$ allows dynamical equilibrium to the system.

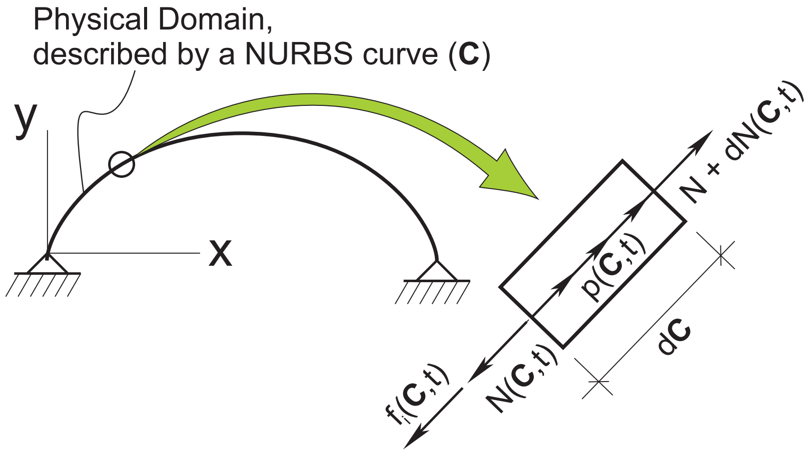

Figure 4: Free body forces for global equilibrium imposing in a curve differencial dC

Imposing dynamical equilibrium in the axis direction in dC and considering the linear expression for axial load $N = AE\epsilon$, where ϵ is the axial strain, the dynamic equilibrium diferencial equation can be writen as:

$$\rho A \frac{\partial^2 \bar{u}}{\partial t^2} - \frac{\partial}{\partial C}\left(EA\frac{\partial \bar{u}}{\partial C}\right) = p(C,t), \tag{6}$$

where ρ is the specific mass, A is the cross sectional area, E the Young Modulus and t the time variable.

Like FEM, IGA expressions are obtained from a variational formulation with same procedures as FEM. Details of variational manipulation for FEM in structural dynamics equations are given by Carey and Oden (1984). Applying the projection of a weight function and the minimization of the residual functional, the general expression for the variational form in a Ω domain of eq. 6 is given by:

$$\int_\Omega \rho A \frac{\partial^2 \bar{u}}{\partial t^2} w \, d\Omega - \int_\Omega \frac{\partial}{\partial C}\left(EA\frac{\partial \bar{u}}{\partial C}\right) w \, d\Omega = \int_\Omega p(C,t) w \, d\Omega, \tag{7}$$

The stiffness term is integrated by parts and the general solution is imposed in the form (Carey and Oden, 1984, Petyt, 2010):

$$\bar{u}(C,t) = e^{i\omega t}u(C). \tag{8}$$

The equation leads 7:

$$\int_{\Omega} \rho A \, uw \, d\Omega - \int_{\Omega} EA \frac{\partial w}{\partial C}\frac{\partial u}{\partial C} \, d\Omega = \int_{\Omega} p(C,t) w \, d\Omega. \tag{9}$$

The dynamical equilibrium equation described in eq. 9 shows respectively the mass, the stiffness and the force terms. For the application of IGA in the equilibrium sentence (eq. 9) the discretization with Galerkin method is considered by write an approximate $\tilde{u}$ field described by a linear combination of NURBS shape functions $R_{i,p}$. Note that, as dicussed in the section above, the discretization proccess in isogeometric analysis is performed in the parametric domain. This leads two basic advantages, related with the possibility of direct global mapping and to describe any global variable, including material properties, in the parametric domain. The displacement field can also be locally described by

$$\tilde{u}(\xi) = \sum_{i=1}^{n} R_{i,p}(\xi)\tilde{u}_i. \tag{10}$$

Replacing the discretization proccess (eq. 10) in eq. 9, the mass, stiffness and force expressions are described in terms of NURBS functions, in a global domain:

$$\mathbf{M} = \int_{C} \rho A \, \mathbf{H}^T \mathbf{H} \, dC, \tag{11}$$

$$\mathbf{K} = \int_{C} EA \, \mathbf{B}^T \mathbf{B}^T \, dC, \tag{12}$$

$$\mathbf{f} = \int_{C} p \, \mathbf{H}^T \, dC, \tag{13}$$

where $\mathbf{H}$ and $\mathbf{B}$ are function vectors:

$$\mathbf{H} = \begin{bmatrix} R_{1,p} & R_{2,p} & \dots & R_{n,p} \end{bmatrix} \tag{14}$$

$$\mathbf{B} = \begin{bmatrix} \frac{\partial R_{1,p}}{dC} & \frac{\partial R_{2,p}}{dC} & \dots & \frac{\partial R_{n,p}}{dC} \end{bmatrix}. \tag{15}$$

The local context can be applied by write dC in function of $d\xi$. The slice dC of the curve $\mathbf{C}$ is written in terms of global coordinates x and y.

$$\frac{\partial C}{\partial \xi} = J(\xi) = \sqrt{\left(\frac{\partial X}{\partial \xi}\right)^2 + \left(\frac{\partial Y}{\partial \xi}\right)^2} \tag{16}$$

It's important to note that eqs. 11, 12 and 13 can be thought as line integrals, where dC is the mapping term. The local definition is applied by replace eq. 16 in the integrals and apply chain rule in the terms of vector $\mathbf{B}$.

Like FEM the standard procedure in IGA is to perform numerical integration by quadrature. As each quadrature point is applied in all matrix elements and the mapping term depends only on ξ. The local form can be written as:

$$\mathbf{M} = \int_0^1 \rho A \, \mathbf{H}^T \mathbf{H} \, J(\xi) \, d\xi, \tag{17}$$

$$\mathbf{K} = \int_0^1 EA \, \hat{\mathbf{B}}^T \hat{\mathbf{B}} \, \frac{1}{J(\xi)} \, d\xi, \tag{18}$$

$$\mathbf{f} = \int_0^1 p \, \mathbf{H}^T \, J(\xi) \, d\xi, \tag{19}$$

where the vector $\hat{\mathbf{B}}$ contains the local derivatives of $R_{i,p}$ given by:

$$\hat{\mathbf{B}} = \begin{bmatrix} \frac{\partial R_{1,p}}{d\xi} & \frac{\partial R_{2,p}}{d\xi} & \dots & \frac{\partial R_{n,p}}{d\xi} \end{bmatrix}. \tag{20}$$

By assuming no external forces acting ($\mathbf{f} = \mathbf{0}$) the problem statement turns into a generalized eigenvalue problem in the form:

$$\mathbf{K}\mathbf{u}^h = \omega_h^2 \mathbf{M}\mathbf{u}^h \tag{21}$$

where ω_h denotes the approximate free vibration frequency related with the i_{th} vibration mode in $\mathbf{u}^h$.

4 GFEM for free vibration response

Several improvements in FEM technique were performed to increase its efficacy. Beyond the different refinement strategies, the extension of FEM space shown positive results in numerical accuracy for structural dynamics in the early works performed by Ganesan and Engels (1992) and Engels (1992). The conception of partition of unity method (Melenk and Babuska, 1996) gave foundations to convergence and stability under a prescript behavior of these additional FEM spaces. The enriched methods based in partition of unity as GFEM , XFEM and PUFEM brought numerical robustness in the enrichment space by the idea to take along the partition of unity space in the enrichment levels. In structural dynamics the advantages of the GFEM strategy compared with other enriched methods was shown by Arndt et al. (2010) and Arndt et al. (2016), including adaptivity techniques.

4.1 Partition of unity

Let a boundary value problem defined on Ω, which its solution is described by $u \in \mathbf{H}(\Omega)$. The domain Ω is divided by an open cover $\{\Omega_i\}$ with an overlap condition given by:

$$\exists M_S \in \mathbf{N} \text{ so that } \forall x \in \mathbf{\Omega} \;\; card\{i|x \in \Omega_i\} \leq M_s. \tag{22}$$

A partition of unity defined on the cover $\{\Omega_i\}$ is a set of functions $\{\eta_i\}$ which presents two specific behaviors, namely:

$$supp(\eta_i) = \{x \in \mathbf{\Omega}|\eta_i(x) \neq 0\} \subset [\Omega_i], \forall i, \tag{23}$$

$$\sum_i \eta_i \equiv 1 \text{ on } \Omega, \tag{24}$$

where $supp(\eta_i)$ denotes the support of the function η_i and $[\Omega_i]$ the closure of the patch Ω_i.

The partition of unity allows to extend the approximated solution space with additional functions $S_i \in \mathbf{H}(\Omega_i \cap \Omega)$ that locally well represents u, in the form:

$$S_i = \left\{s_i^j\right\}_{j=1}^{m} \tag{25}$$

The enriched set is defined by multiplying each enrichment function s_i^j by the partition function η_i. The enrichment space is defined as:

$$S := \sum_{i=1} \eta_i S_i = \left\{\sum_i \eta_i s_i^j\right\} \subset \mathbf{H}(\mathbf{\Omega}). \tag{26}$$

The approximate enriched solution for u is so described by:

$$u_h(x) = \sum_i \sum_{s_i^j \in S_i} \eta_i s_i^j(x) a_{ij}, \tag{27}$$

where a_{ij} denotes the degrees of freedom of the problem.

4.2 Enrichment functions

A formulation of GFEM applied to free vibration analysis of straight bars and trusses was developed by Arndt et al. (2010) in which shown efficacy with trigonometrical enrichment functions. The enrichment space proposed by Arndt et al. (2010) depends on the number of enrichment levels n_l and is given by:

$$S_i = \left\{ 1 \quad \gamma_{1j} \quad \gamma_{2j} \quad \phi_{1j} \quad \phi_{2j} \quad \ldots \right\}, \quad j = 1, 2, 3, \ldots, n_l, \tag{28}$$

where in the element domain, with parametric coordinates on ξ, the enrichment functions are given by:

$$\gamma_{1j} = \sin(\beta_j L_e \xi) \tag{29}$$

$$\gamma_{2j} = \sin(\beta_j L_e (\xi - 1)) \tag{30}$$

$$\phi_{1j} = \cos(\beta_j L_e \xi) - 1 \tag{31}$$

$$\phi_{2j} = \cos(\beta_j L_e (\xi - 1)) - 1 \tag{32}$$

with

$$\beta_j = \sqrt{\frac{\rho}{E}} \mu_j, \tag{33}$$

where L_e is the element length in FEM concept, ρ is the specific mass, E the Young modulus and μ_j is the frequency related with the j_{th} enrichment level. Note that β_j could depend on ξ in non-homogeneous conditions. Figure 5 represents an example of these functions behavior for $L_e = 1$ and $\beta_j = 3\pi/2$.

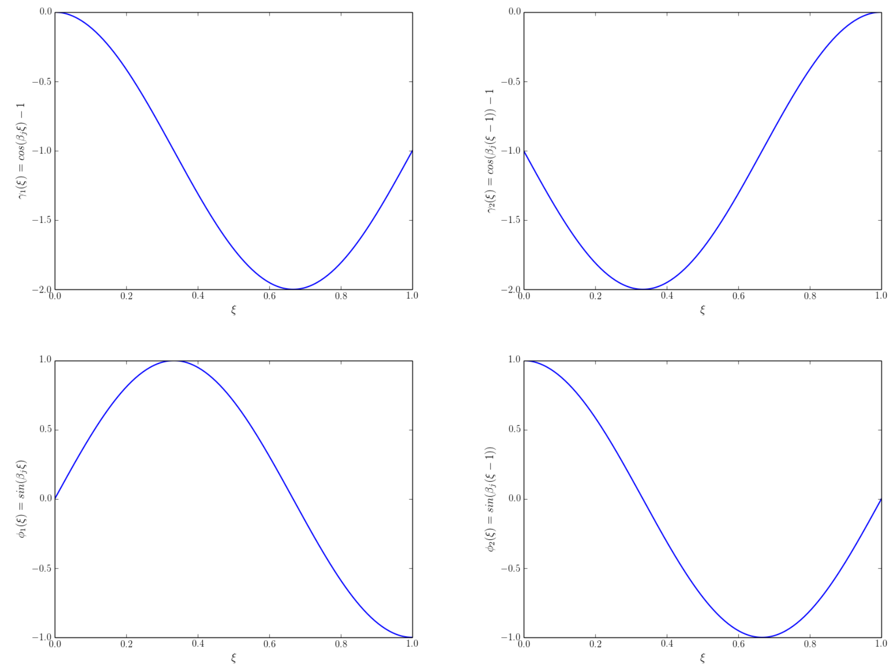

Figure 5: Trigonometric enrichment functions with $\beta_j = 3\pi/2$

The partition of unity used in the examples developed by Arndt et al. (2010) is the set of linear shape functions defined on the unitary domain as:

$$\eta_1(\xi) = 1 - \xi \tag{34}$$

$$\eta_2(\xi) = \xi \tag{35}$$

The product between the partition of unity functions with the enrichment functions must be performed taking care to ensure prescript boundary conditions, i.e the resultant enriched functions by partition of unity should also vanish at the boundaries. By this condition the function space with the enrichment levels is given by:

$$S = \left\{ \eta_1 \quad \eta_2 \quad \gamma_{1j}\eta_1 \quad \phi_{1j}\eta_1 \quad \gamma_{2j}\eta_2 \quad \phi_{2j}\eta_2 \quad \ldots \right\}, \;\; j = 1, 2, 3, \ldots, n_l, \tag{36}$$

5 Enriched NURBS formulation

An unified formulation between isogeometric analysis and the enriched concept is discussed. Since the enrichment functions can be also defined on the parametric space, an enrichment function which presents a global behavior can be defined on the local space. Aiming numerical experiments the mapping capabilities on the NURBS conception is tested concerning two basic partition of unity spaces on the enriched fields. First the same NURBS partition of unity space used in the geometrical description is considered, i.e:

$$\eta_i = R_{i,p} \tag{37}$$

with enrichment functions given by:

$$\gamma_{1j} = \sin(beta_j L\xi) \tag{38}$$

$$\phi_{1j} = \cos(beta_j L\xi), \tag{39}$$

where L denotes the line integral on the curve $\mathbf{C}(\xi)$.

The second possibility is to test other partition of unity space in the enrichment levels. In this case the same function set in eq. 32 (Arndt et al., 2010) are performed under CAD mapping with partition of unity by simple linear functions (eq. 35).

The fundamental tensors in eqs. 17, 18 and 19 developed with pure isogeometric concept are extended with the enrichment concept by:

$$\mathbf{M} = \int_0^1 \rho A \, \bar{\mathbf{H}}^T \bar{\mathbf{H}} \; J(\xi) \, d\xi, \tag{40}$$

$$\mathbf{K} = \int_0^1 EA \, \bar{\mathbf{B}}^T \bar{\mathbf{B}} \; \frac{1}{J(\xi)} \, d\xi, \tag{41}$$

$$\mathbf{f} = \int_0^1 p\, \bar{\mathbf{H}}^T\, J(\xi)\, d\xi, \tag{42}$$

The conception of extended tensors depends on enrichment strategy. First by NURBS enrichment the tensors are described by:

$$\bar{\mathbf{H}} = \begin{bmatrix} R_{1,p} & \dots & R_{n,p} & \phi_i j R_{1,p} & \dots & \phi_i R_{n,p} & \dots \end{bmatrix}, \quad i = 1, 2, \dots, n_l \tag{43}$$

$$\bar{\mathbf{B}} = \begin{bmatrix} \frac{\partial R_{1,p}}{\partial \xi} & \dots & \frac{\partial R_{n,p}}{\partial \xi} & \frac{\partial \phi_i R_{1,p}}{\partial \xi} & \dots & \frac{\partial \phi_i R_{n,p}}{\partial \xi} & \dots \end{bmatrix}, \quad i = 1, 2, \dots, n_l \tag{44}$$

The NURBS based enrichment with GFEM functions (Arndt et al., 2010) is given by:

$$\bar{\mathbf{H}} = \begin{bmatrix} R_{1,p} & \dots & R_{n,p} & \eta_1\gamma_{1j} & \eta_1\phi_{1j} & \eta_2\gamma_{2j} & \eta_2\phi_{2j} & \dots \end{bmatrix}, \quad j = 1, 2, \dots, n_l \tag{45}$$

$$\bar{\mathbf{B}} = \begin{bmatrix} \frac{\partial R_{1,p}}{\partial \xi} & \dots & \frac{\partial R_{n,p}}{\partial \xi} & \frac{\partial \eta_1\gamma_{1j}}{\partial \xi} & \frac{\partial \eta_1\phi_{1j}}{\partial \xi} & \frac{\partial \eta_2\gamma_{2j}}{\partial \xi} & \frac{\partial \eta_2\phi_{2j}}{\partial \xi} & \dots \end{bmatrix}, \quad j = 1, 2, \dots, n_l. \tag{46}$$

6 Adaptive Strategy

The adaptive strategy, also developed by Arndt et al. (2010) for free vibration analysis, consists to choose a target frequency, where this target represents a vibration mode that wish to be well approximate. In the first step of the process, a pure FEM analysis is performed and the resultant target frequency is used to perform the first enriched analysis with GFEM, where this target frequency adjusts the β parameter. GFEM procedure is repeated until the target frequency reach some convergence test. The last resultant target frequency obtained by GFEM refeeds the new procedure. In this case the enrichment involves only one level. Figure 6 represents a schematic idea of the whole adaptive proccess.

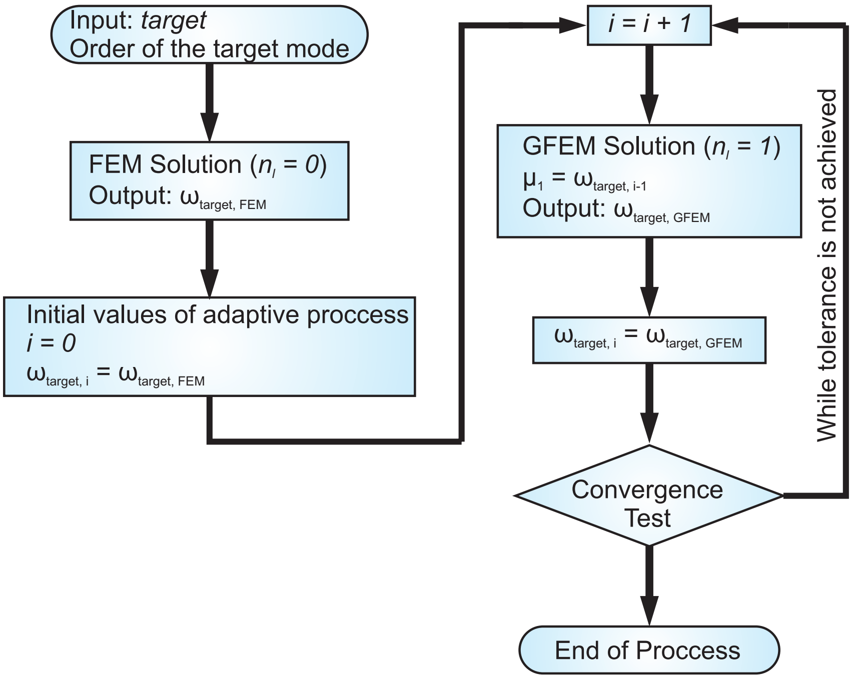

Figure 6: Adaptive GFEM flowchart proposed by Arndt et al. (2010)

7 Numerical Experiments

7.1 Homogeneous Unitary Bar

The first experiment is to test efficacy of pure functions neglecting the effect of mapping on a homogeneous unitary bar with properties given in fig. 7.

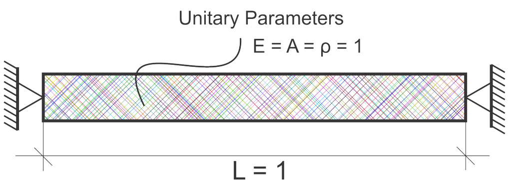

Figure 7: Unitary bar

This problem has its free vibration frequencies analytically described by:

$$\omega_i = \pi i \quad \text{with} \quad i = 1, 2, 3, \ldots \tag{47}$$

Figure 8 shows the relative error on vibration frequencies for the adaptive process, where these errors are put in function of iterations number on adaptive process.

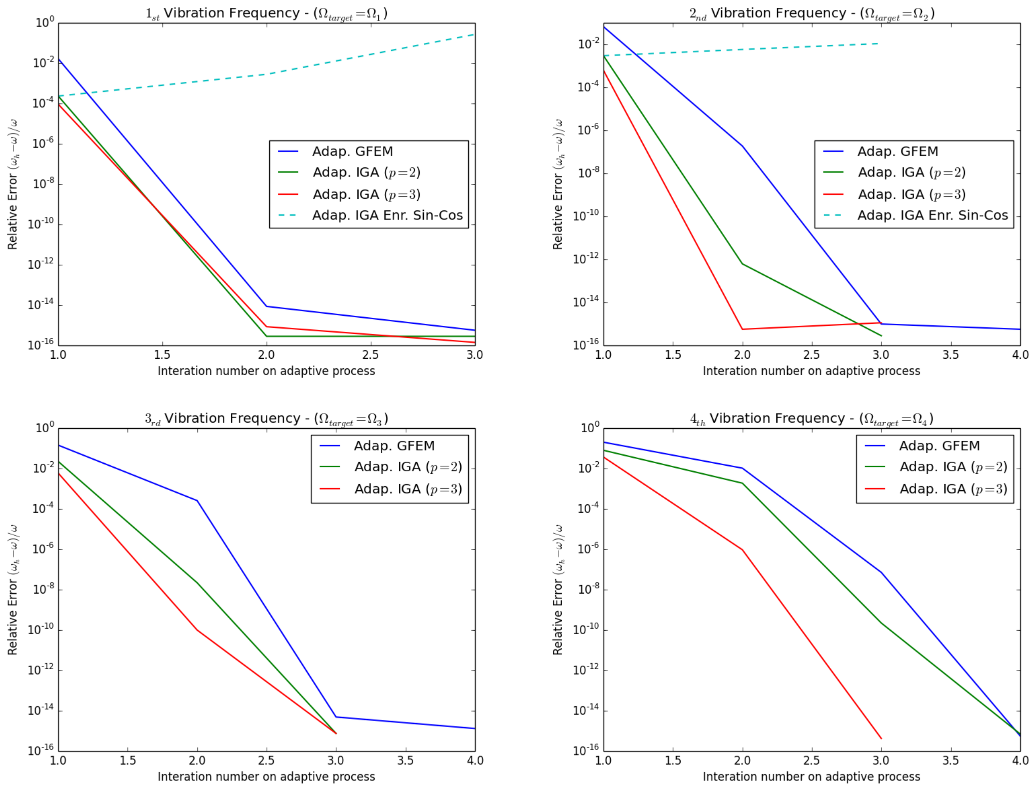

Figure 8: Relative error in function of number of iterations for the first 4 vibration frequencies

7.2 Heterogeneous Bar

In this section the presented formulations of the enriched are tested through the free vibration of a non-homogeneous bar (fig. 9) with two materials. The left boundary is restrained and the right maintains with freedom.

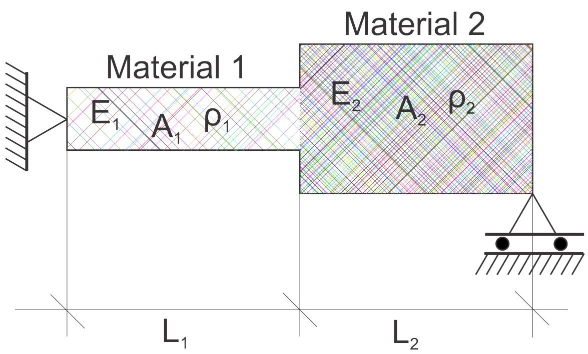

Figure 9: Two materials bar

The analytical solution was developed by Arndt (2009) which obtained a non-linear condition for exact frequency field:

$$E_1 A_1 \kappa_1 \cos(\kappa_1 L_1) \cos(\alpha \kappa_1 L_2) - \alpha E_2 A_2 \kappa_1 \sin(\kappa_1 L_1) \sin(\alpha \kappa_1 L_2) = 0 \tag{48}$$

An analysis is performed considering $L_1 = L_2 = 1.$, $E_1 = 1.$, $A_1 = 1.$, $\rho_1 = 1.$, $E_2 = 2.$, $A_2 = 2.$, $\rho_2 = 8.$. As the length parameters are set as equal, a set of parametric functions which expresses the material conditions can be used to facilitate the integration process, as those properties can be directly considered in the parametric domain. These material functions are shown in fig. 10, where the mass, elasticity and cross sectional area are draw.

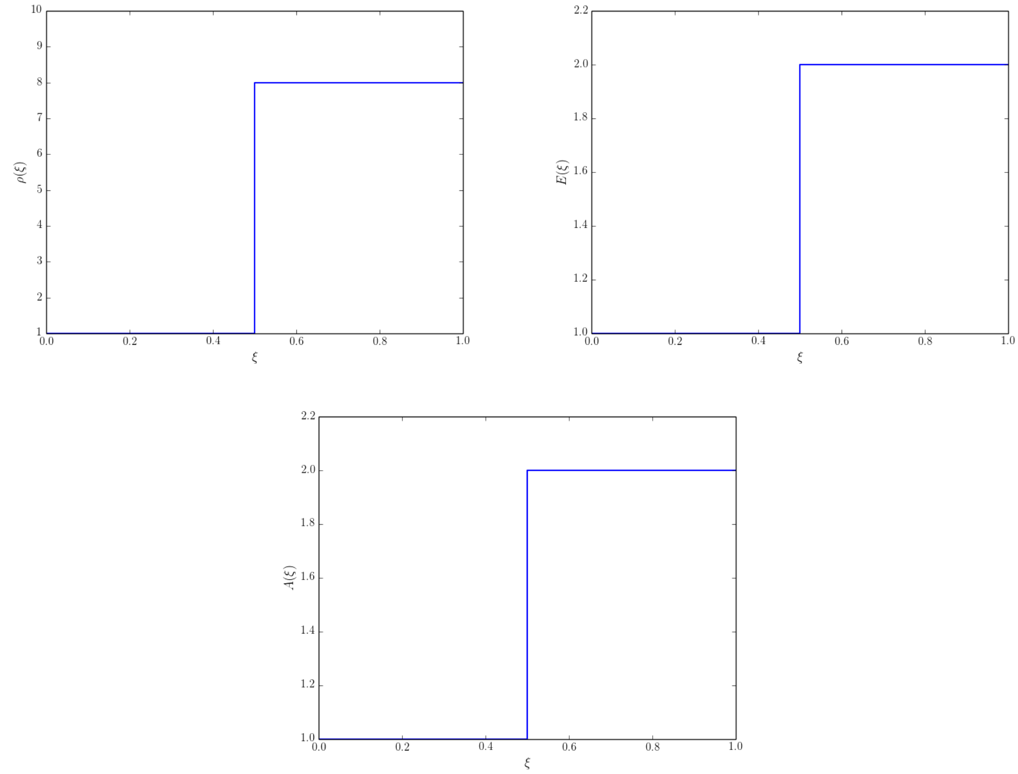

Figure 10: Global material properties defined on the parametric space

7.3 Pure Isogeometric Results

The pure isogeometric solution is performed in a element-wise k refinement, maintaining C^0 continuity at the middle knot, the elementary shape functions used in the problem are shown in fig. 11. The same set is also used as partition of unity. The geometry parameters related with CAD mapping are inputed by:

$$\mathbf{B}_i = \begin{bmatrix} X_i \\ Y_i \end{bmatrix} = \begin{bmatrix} 2(i-1)/(n-1) \\ 0 \end{bmatrix} \tag{49}$$

,

$$w_i = 1, \tag{50}$$

where $i = 1, \ldots, n$ and n denotes the number of shape functions.

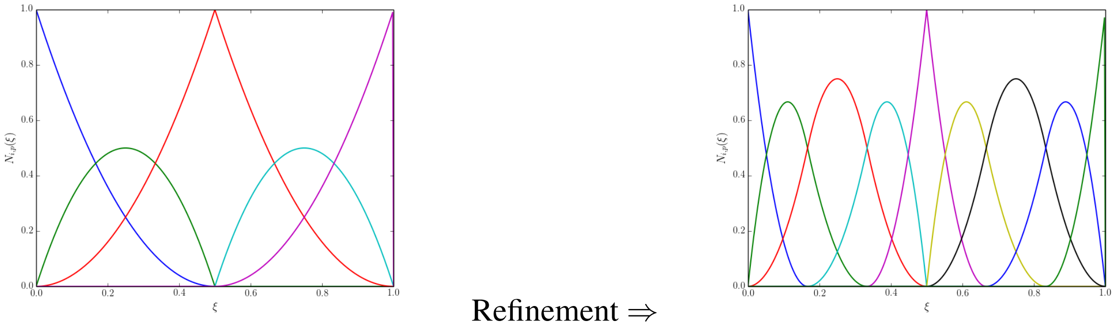

Figure 11: The b-splines refinement scheme in the problem

The frequency field obtained with isogeometric approach is normalized with the analytical solution in function of the mode number normalized with the total number on degrees of freedom. Figure 12 shows a comparison of the frequency error spectra for polynomial degrees $p = 2, \ldots, 5$.

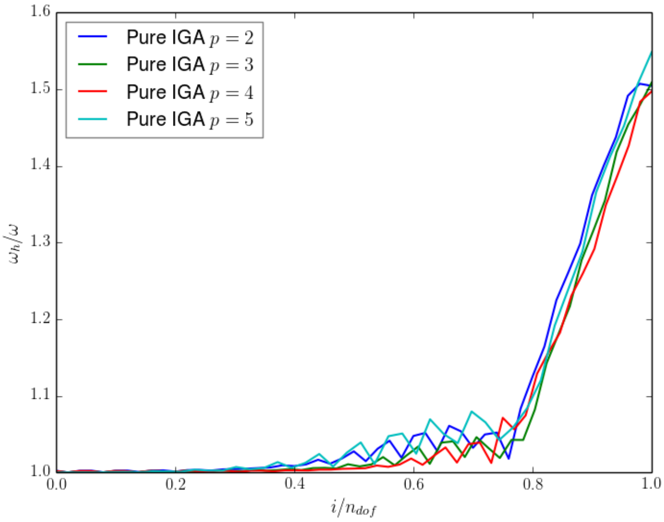

Figure 12: Frequency error spectra for pure isogeometric analysis

The results shows a acceptable accuracy for 40% of the sample, being the graphics built with 80 degrees of freedom.

7.4 Enriched NURBS Results

A partition of unity composed by b-splines with degree $p = 2$ and $n = 10$ is chosen. Figure 13 shows the frequency spectra comparing FEM, pure IGA and two enriched versions with parameters $\mu_1 = \pi$ and $\mu_1 = \pi/2$. presenting only one enrichment level.

Table 1: Relative percentual errors on vibration frequencies

i	Lin. FEM	IGA $p = 2$	IGA $p = 4$	Enr. IGA $\mu_1 = \pi/2.$	Enr. IGA $\mu_1 = \pi$
1	0.21544488	0.227183943	1.72649141e-02	**0.0**	0.19708266
2	0.73057115	1.67806400e-03	5.58219385e-02	1.00286717e-02	0.08795314
3	0.2607921	2.27112316e-01	3.32551198e-03	5.31038689e-02	0.07212039
4	0.52026093	2.34471809e-01	3.50403521e-02	8.72072965e-02	0.5136656
5	0.22339411	1.60479972e-02	6.99285114e-02	5.38192461e-01	0.11478192
6	0.71942815	2.35829059e-01	2.66828988e-02	2.79196607e-01	6.05228441

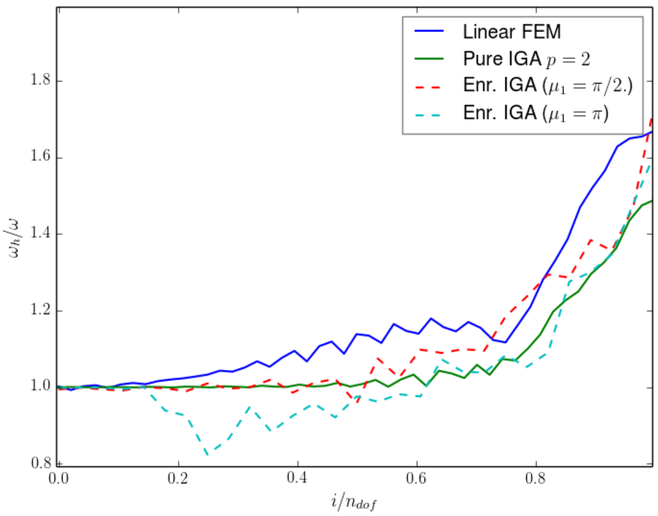

Figure 13: Frequency error spectra for FEM, pure and enriched IGA

For the verification of convergence on the example, table 1 shows the percentual relative errors on the frequency field.

8 CONCLUSIONS

This paper presented an enriched formulation with adaptivity in the isogeometric point of view. The first experiments involving the unitary bar a high convergence is observed in GFEM and enriched NURBS with Arndt's functions. Is also observed that *k* refinement can improve the convergence on adaptive process.

Is also observed in the unitary bar experiment that NURBS with enriched sine and cosine functions is not capable to present an adaptive behavior. But the experiment involving non homogeneous bar shows a capability of those functions to describe exact frequencies from the parametric space.

Concerning the pure isogeometric concept, the results shows an accuracy of 40% of the sample, presenting also a homogeneous spectra behavior in function of polynomial degree.

REFERENCES

Arndt, M. (2009), O Método dos Elementos Finitos Generalizados Aplicado À Análise de Vibrações Livres de Estruturas Reticuladas, PhD thesis, Programa de Pós-Graduação em Métodos Numéricos em Engenharia, Curitiba. Doutorado em Método Numéricos em Engenharia.

Arndt, M., Machado, R. D. and Scremin, A. (2010), 'An adaptive generalized finite element method applied to free vibration analysis of straight bars and trusses', *Journal of Sound and Vibration* **329**, 659–672.

Arndt, M., Machado, R. D. and Scremin, A. (2011), *Advances in Vibration Analysis Research*, Intech, chapter The Generalized Finite Element Method Applied to Free Vibration of Framed Structures, pp. 187–212.

Arndt, M., Machado, R. D. and Scremin, A. (2016), 'Accurate assessment of natural frequencies for uniform and non- uniform Euler-Bernoulli beams and frames by adaptive generalized finite element method', *Engineering Computations* **33**(5).

Benson, D. J., Bazilevs, Y., Hsu, M. C. and Hughes, T. J. R. (2010a), 'Isogeometric shell analysis: The Reissner-Mindlin shell', *Computer Methods in Applied Mechanics and Engineering* **199**(5-8), 276–289.

Carey, G. F. and Oden, J. T. (1984), *Finite Element: Computational Aspects*, Prentice Hall, New Jersey.

Cottrell, J. A., Hughes, A. T. J. R. and Reali, A. (2007), 'Studies of refinement and continuity in isogeometric structural analysis', *Computer Methods in Applied Mechanics and Engineering* **196**, 4160–4183.

Cottrell, J. A., Reali, A., Bazilevs, Y. and Hughes, T. J. R. (2006), 'Isogeometric analysis of structural vibrations', *Computer Methods in Applied Mechanics and Engineering* **195**, 5257–5196.

De-Boor, C. (1972), 'On calculation of b-splines', *Journal of Approximation Theory* **6**, 50–62.

Engels, R. C. (1992), 'Finite element modeling of dynamic behavior of some basic structural members', *Journal of Vibration and Acoustics* **114**, 3–9.

Farin, G. (n.d.), *Curves and Surfaces for CAGD: a practical guide*, 5th edition edn, Academic Press.

Farin, G. E. (1999), *NURBS: from projective geometry to practical use*, 2 edn, A K Peters, Natick.

Ganesan, N. and Engels, C. (1992), 'Hierarchical bernoulli-euller beam finite elements', *Computer & Structures* **43**(2), 297–304.

Ghorashi, S. S., Valizadeh, N. and Mohammadi, S. (2011), 'X-FEM in isogeometric analysis for linear fracture mechanics', *International Journal for Numerical Methods in Engineering* **89**, 1069–1101.

Hughes, T. J. R., Cottrell, J. A. and Bazilevs, Y. (2005), 'Isogeometric analysis: Cad, finite elements, nurbs, exact geometry and mesh refinement', *Computer Methods in Applied Mechanics and Engineering* **194**, 4135–4195.

Luycker, E. D., Benson, D. J., Belytschko, T. and Hsu, Y. B. M. C. (2011), 'X-FEM in isogeometric analysis for linear fracture mechanics', *International Journal for Numerical Methods in Engineering* **87**, 541–565.

Melenk, J. M. and Babuska, I. (1996), 'The partition of unity finite element method: Basic theory and applications', *Computer methods in applied mechanics and engineering* **139**, 289–314.

Petyt, M. (2010), *Finite Element Vibration Analysis*, 2 edn, Cambridge University Press, Cambridge.

Piegl, L. and Tiller, W. (1997), *The NURBS Book*, Springer-Verlag, Germany.

Rauen, M., Machado, R. D. and Arndt, M. (2017), 'Isogeometric Analysis of Free Vibration of Framed Structures : Comparative Problems', *Engineering Computations* **34**(2).

Shojaee, S., Valizadeh, N., Izadpanah, E., Bui, T. and Vu, T. V. (2012), 'Free vibration and buckling analysis of laminated composite plates using the NURBS-based isogeometric finite element method', *Composite Structures* **94**(5), 1677–1693.

Thai, C. H., Nguyen-Xuan, H., Nguyen-Thanh, N., Le, T.-H., Nguyen-Thoi, T. and Rabczuk, T. (2012), 'Static, free vibration, and buckling analysis of laminated composite ReissnerâĂŞ-Mindlin plates using NURBS-based isogeometric approach', *International Journal for Numerical Methods in Engineering* .

Torii, A. J., Machado, R. D. and Arndt, M. (2015), 'GFEM for modal analysis of 2D wave equation', *Engineering Computations* **32**(6), 1779–1801.